

## **Forum**

# Dead or alive: carbon as a currency to integrate disease and ecosystem ecology theory

Eric W. Seabloom<sup>®</sup><sup>1</sup>, Angela Peace<sup>2</sup>, Lale Asik<sup>3</sup>, Rebecca A. Everett<sup>4</sup>, Thijs Frenken<sup>®5,6</sup>, Angélica L. González<sup>7</sup>, Alexander T. Strauss<sup>1,8,9,10</sup>, Dedmer B. Van de Waal<sup>5</sup>, Lauren A. White<sup>®11</sup> and Elizabeth T. Borer<sup>1</sup>

Correspondence: Eric W. Seabloom (seabloom@umn.edu)

Oikos 2023: e09880 doi: 10.1111/oik.09880

Subject Editor: Dries Bonte Editor-in-Chief: Dries Bonte Accepted 6 March 2023





www.oikosjournal.org

Death is a common outcome of infection, but most disease models do not track hosts after death. Instead, these hosts disappear into a void. This assumption lacks critical realism, because dead hosts can alter host-pathogen dynamics. Here, we develop a theoretical framework of carbon-based models combining disease and ecosystem perspectives to investigate the consequences of feedbacks between living and dead hosts on disease dynamics and carbon cycling. Because autotrophs (i.e. plants and phytoplankton) are critical regulators of carbon cycling, we developed general model structures and parameter combinations to broadly reflect disease of autotrophic hosts across ecosystems. Analytical model solutions highlight the importance of disease-ecosystem coupling. For example, decomposition rates of dead hosts mediate pathogen spread, and carbon flux between live and dead biomass pools are sensitive to pathogen effects on host growth and death rates. Variation in dynamics arising from biologically realistic parameter combinations largely fell along a single gradient from slow to fast carbon turnover rates, and models predicted higher disease impacts in fast turnover systems (e.g. lakes and oceans) than slow turnover systems (e.g. boreal forests). Our results demonstrate that a unified framework, including the effects of pathogens on carbon cycling, provides novel hypotheses and insights at the nexus of disease and ecosystem ecology.

Keywords: decomposition, disease ecology, ecosystem ecology, pathogen, transmission

<sup>&</sup>lt;sup>1</sup>Dept of Ecology, Evolution, and Behavior, Univ. of Minnesota, St. Paul, MN, USA

<sup>&</sup>lt;sup>2</sup>Dept of Mathematics and Statistics, Texas Tech Univ., Lubbock, TX, USA

<sup>&</sup>lt;sup>3</sup>Dept of Mathematics and Statistics, Univ. of the Incarnate Word, TX, USA

<sup>&</sup>lt;sup>4</sup>Dept of Mathematics and Statistics, Haverford College, Haverford, PA, USA

<sup>&</sup>lt;sup>5</sup>Dept of Aquatic Ecology, Netherlands Inst. of Ecology, Wageningen, the Netherlands

<sup>&</sup>lt;sup>6</sup>Great Lakes Inst. for Environmental Research, Univ. of Windsor, Windsor, ON, Canada

<sup>&</sup>lt;sup>7</sup>Dept of Biology and Center for Computational and Integrative Biology, Rutgers Univ., Camden, NJ, USA

<sup>&</sup>lt;sup>8</sup>Odum School of Ecology, Univ. of Georgia, Athens, GA, USA

Center for the Ecology of Infectious Diseases, University of Georgia, Athens, GA, USA

<sup>&</sup>lt;sup>10</sup>River Basin Center, University of Georgia, Athens, GA, USA

<sup>&</sup>lt;sup>11</sup>Natl Socio-Environmental Synthesis Center, Univ. of Maryland, Annapolis, MD, USA

<sup>© 2023</sup> The Authors. Oikos published by John Wiley & Sons Ltd on behalf of Nordic Society Oikos.

This is an open access article under the terms of the Creative Commons Attribution License, which permits use, distribution and reproduction in any medium, provided the original work is properly cited.

#### Introduction

Host–pathogen interactions occur within an ecosystem context (Preston et al. 2016, Borer et al. 2021a), with nutrient supply rates, climate, and biodiversity altering the outcome of many host–pathogen interactions (Keesing et al. 2006, Seabloom et al. 2015, Borer et al. 2016). In turn, pathogens can be important drivers of ecosystem fluxes, such as primary productivity, decomposition, and nutrient cycling, because they can alter host growth and death rates and tissue chemistry (Mitchell 2003, Suttle 2005, Lovett et al. 2010, Cobb et al. 2013, Jover et al. 2014, Preston et al. 2016, Seabloom et al. 2017, Fischhoff et al. 2020). Despite repeated calls for stronger conceptual linkages (Loreau et al. 2005, Preston et al. 2016), theoretical advances in disease and ecosystem ecology remain largely separate (Borer et al. 2021a, 2022).

This separation between disease and ecosystem ecology reflects the different conceptualization of live and dead matter in these fields, which leads to use of different currencies. The canonical models in disciplines rooted in population biology, such as disease ecology, are typically formulated in units of individuals and use an open framework in which dead individuals permanently exit the system (Keeling and Rohani 2008), perhaps after a period as infectious cadavers (Fuller et al. 2012). In contrast, the movement of matter and energy between living and non-living states lies at the core of ecosystem ecology, and ecosystem models are typically formulated in units of elemental mass (e.g. carbon) or energy that can be tracked as they flux between biotic and abiotic states (Lindeman 1942, Pastor 2008).

Population-based models have formed the core of theory in disease ecology since the inception of the field (Kermack et al. 1927, May and Anderson 1979, Heesterbeek and Roberts 2015), and this tight coupling with theory has facilitated rapid conceptual advances and links with fields such as community ecology (Holt and Pickering 1985, May and Nowak 1994, Keesing et al. 2006, Seabloom et al. 2015, Borer et al. 2016) and behavioral ecology (Madden et al. 2000, Ezenwa et al. 2016, Verelst et al. 2016, Shaw et al. 2017, Brookes et al. 2019, Shoemaker et al. 2019, Strauss et al. 2020). However, population-based models have hindered progress in developing an integrated theoretical framework for disease and ecosystem ecology. While population-based models in disease ecology have examined the effects of abiotic resources (e.g. nitrogen or phosphorus) on population, community, and disease dynamics (Borer et al. 2016, Pell et al. 2019, Strauss et al. 2019), the matter that comprises the hosts in these models is not typically tracked after hosts die and decompose. Nevertheless, dead hosts can have significant effects on the host, and pathogen dynamics (e.g. host growth rates and pathogen spread), and their fate determines critical ecosystem fluxes (e.g. decomposition rates and microbial respiration).

Dead hosts can alter host and pathogen dynamics by serving as sources of infectious pathogen propagules (Breban et al. 2009, Fuller et al. 2012, Thingstad et al. 2014) or through effects on host growth and death rates (Foster and Gross 1998, Clark and Tilman 2010). For example, dead primary producer biomass (i.e. litter or necromass) can increase the impacts of fungal pathogens on plant seedlings (García-Guzmán and Benítez-Malvido 2003, Beckstead et al. 2012). In addition, dead primary producer biomass, such as leaf litter in forests or wrack in saltmarshes, can reduce plant growth and reproduction through shading or by creating a physical barrier to growth (Shigesada and Okubo 1981, van der Valk 1986, Bertness and Ellison 1987, Townsend et al. 1994, Brewer et al. 1998, Foster and Gross 1998, Clark and Tilman 2010, Flynn and Raven 2017). In the longer term, nutrients from dead primary producer hosts can be recycled potentially increasing host growth (Weil and Magdoff 2004, Pastor 2008, Chapin et al. 2012, Schlesinger and Bernhardt 2013, Klawonn et al. 2021). This feedback has been well studied in marine systems, where viral lysis of microbial hosts can increase organic matter recycling and net primary productivity (i.e. the viral shunt; Wilhelm and Suttle 1999, Weitz et al. 2015).

In contrast to disease ecology, models in ecosystem ecology are typically formulated in currencies of energy and elements (e.g. mass of carbon or nitrogen), which can be tracked as they move between living and non-living ecosystem compartments (Lindeman 1942, Chapin et al. 2012, Schlesinger and Bernhardt 2013). However, these types of ecosystem models have rarely included pathogens (Weitz et al. 2015, Vage et al. 2016, Borer et al. 2021a, 2022), although ecosystem ecology has long recognized the primacy of microbes in regulating some fluxes of energy and elements (e.g. decomposition and microbial respiration, Roy et al. 2001, Chapin et al. 2012, Schlesinger and Bernhardt 2013). Nevertheless, microbial pathogens can directly affect ecosystem fluxes and pools by altering the fixation of carbon (C) through photosynthesis (e.g. gross primary productivity), respiration, and host mortality and the supply of organic C to decomposers (Wilhelm and Suttle 1999, Suttle 2007, Preston et al. 2016, Kohli et al. 2019, Cappelli et al. 2020, Borer et al. 2021a, Kohli et al. 2021).

Here we develop a theoretical framework using carbon as currency to integrate disease and ecosystem modeling approaches to investigate feedbacks between disease and ecosystem dynamics. This framework is composed of a series of four carbon-based models: 1) a logistic-growth model, 2) a disease model, 3) an ecosystem model, and 4) an integrated disease-ecosystem model (Fig. 1). By formulating these models in units of elemental carbon (g C), we can directly track fluxes of matter between biotic and abiotic states (Pastor 2008, Borer et al. 2021a). We focus on pathogens of autotrophs (e.g. primary producers such as plants and phytoplankton), as these hosts regulate ecosystem carbon fluxes between organic and inorganic material states through photosynthesis, respiration, and decomposition (Chapin et al. 2012). In addition to their unique role as the primary source of energy for most food webs, autotrophs dominate organic ecosystem carbon; they comprise over 80% of biomass on Earth, with microbes accounting for an additional 19% (Bar-On et al. 2018).

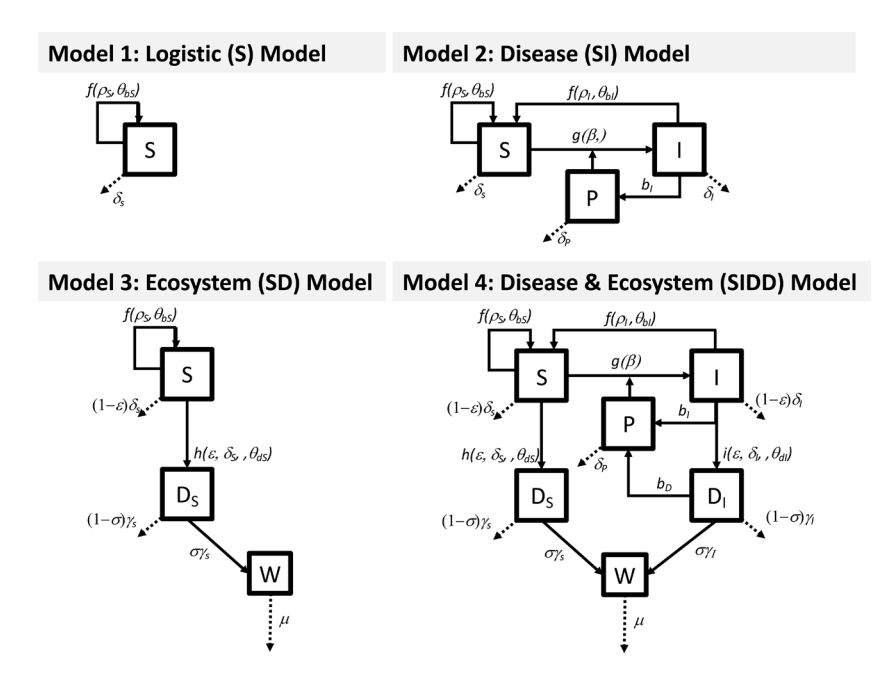


Figure 1. Schematic of nested ecosystem and disease models. Parameters are described in text and in the Supporting information.

Our goal here is to develop a general, discipline-bridging framework that produces parameter-independent, analytical solutions, thereby increasing generality over more complex models that require simulation-based analyses of finite regions of parameter space. This approach builds from ecosystemspecific models, which include greater system-level realism at the cost of generality (Ruardij et al. 2005, Jacquet et al. 2010, Rhodes and Martin 2010, Weitz et al. 2015, Vage et al. 2016). By formulating models with closed-form solutions expressed in terms of interpretable biological processes (e.g. decomposition rate), the approach can reveal general, biologically meaningful insights that are independent of specific ranges or combinations of parameters. We then use these models to build links among earlier system-specific models by exploring model dynamics around biologically relevant parameter values and combinations that broadly align with organisms and process rates in different ecosystem types (e.g. terrestrial, freshwater and marine).

In related work, Borer et al. (2021a, 2022) developed and analyzed stoichiometric models linking ecosystem and disease ecology to examine the concurrent fluxes and recycling of carbon and a growth-limiting nutrient (e.g. nitrogen or phosphorus). These stoichiometric models that explicitly include the effects of environmental nutrients on host growth are well-suited for examining dynamics arising from elemental recycling. However, because of their greater complexity, analyses of these models cannot be parameter value independent; insights rely on simulations of finite parameter sets. The carbon-based models presented here sacrifice some realism of earlier approaches but gain the greater generality that arises from analytical solutions. These carbon-based models also have fewer parameters than stoichiometric models, making it possible to parameterize our model to visualize dynamics across a broader range of biologically motivated parameter

value combinations than the earlier stoichiometric ecosystem-disease (Borer et al. 2021a, 2022). Finally, by focusing on carbon in the current model, we can include additional pools of carbon that are important in a wide range of host–pathogen systems (e.g. necromass, decomposed carbon, and environmental pools of pathogens, Ruardij et al. 2005, Breban et al. 2009, Fuller et al. 2012, Weitz et al. 2015, Vage et al. 2016).

We use a carbon-based framework to investigate how pools of living and non-living carbon can alter host-pathogen interactions (e.g. pathogen prevalence and spread rates) and how disease can alter important ecosystem properties (e.g. pools of live, dead, and fully decomposed C). We start by examining the analytical equilibria in disease models with and without ecosystem feedbacks (model 2 and 3) and ecosystem models with and without disease (model 3 and 4). We then examine these interactions within biologically relevant parameter values and combinations by estimating parameter values from a range of aquatic, marine and terrestrial biomes (e.g. lakes, oceans, grasslands and forests).

# **Modeling framework**

Here, we present and compare four carbon-based models: 1) a logistic-growth model, 2) a disease model, 3) an ecosystem model and 4) an integrated disease—ecosystem model (Fig. 1). Detailed descriptions of the methods and additional analysis of these models are presented in the Supporting information. Parameter definitions and units are presented in Table 1, and diagrams of the main models are shown in Fig. 1. In these models, we include an environmental pool of pathogens (P). We present a parallel analysis of these models without the explicit environmental pathogen pool in the Supporting information.

Table 1. Parameter units, values (mean and range) and definitions. NAs indicate parameters that are not considered in most disease or ecosystem models. Biome specific parameter values are presented in the Supporting information. \*Used to derive model parameters (Supporting information), but not parameters in the model themselves.

Parameter	Units	Mean value (Range)	Meaning: disease ecology	Meaning: ecosystem ecology
NEP*	g C m <sup>-2</sup> day <sup>-1</sup>	2.39 (0.148–10.8)	NA	Net ecosystem productivity (typically measured in intact ecosystems, i.e. under conditions of light limitation and herbivory)
K*	$g C m^{-2}$	4390 (1–18 300)	Carrying capacity of all hosts in terms of carbon, including live and recently dead biomass [terrestrial] or dead phytoplankton in photic zone [aquatic])	Storage pool of all autotroph carbon (live and recently dead)
r *	day <sup>-1</sup>	0.787 (0.00036–3)	Intrinsic growth rate of hosts	Maximum per carbon NEP under absence of light limitation
α	$m^2\;g\;C^{-1}$	0.204 (0.0000162–0.979)	Strength of density dependence on population growth	Strength of density dependence (i.e. light limitation) on NEP
$\delta_S$	day <sup>-1</sup>	0.0257 (0.0014–0.05)	Per capita death rate for susceptible hosts (litterfall and root turnover [terrestrial ecosystems] or phytoplankton death rate [aquatic])	Litterfall; root turnover; senescence on per carbon basis
$\delta_I$	day <sup>-1</sup>	0.438 (0.0238–0.85)	Per capita death rate for infected hosts	NA
$\rho_S$	day <sup>-1</sup>	0.813 (0.00178–3.05)	Per capita birth rate for susceptible hosts	Net primary productivity rate on per carbon basis
$\rho_I$	day <sup>-1</sup>	0.569 (0.00125–2.14)	Per capita birth rate for infected hosts	NÅ
γs	day <sup>-1</sup>	0.0888 (0.02–0.2)	NA	Decomposition rate for dead susceptible hosts (terrestrial ecosystems) or sinking rate for dead phytoplankton (aquatic)
$\gamma_I$	day <sup>-1</sup>	0.0888 (0.02-0.2)	NA	1 / 1
σ	unitless	0.9	NA	Retention of solid carbon during transition from dead to decomposed pool
ε	unitless	0.9	NA	Retention of solid carbon during transition from live to dead pool
μ	day <sup>-1</sup>		NA	Respiration of solid carbon during transition from dead to decomposed pool
β	$m^2 g C^{-1} day^{-1}$	0.237 (0.00000201–1.33)	Pathogen transmission coefficient	NA
$b_{l}$	day <sup>-1</sup>	$1.9 \times 10^{-4} (1.46 \times 10^{-9} - 0.008)$	Pathogen shedding rate from live infected hosts	NA
$b_{\scriptscriptstyle D}$	day <sup>-1</sup>	$3.35 \times 10^{-5} (1.46 \times 10^{-9} - 0.001)$	Pathogen shedding rate from dead infected hosts	NA
$\delta_p$	day <sup>-1</sup>	0.1449 (0.0013–5)	Environmental pathogen degradation rate	NA
κ	unitless	0	Infectious dose: amount of pathogen incorporated into host during infection	NA

In the following models, the basic reproduction number of the pathogen  $(R_0)$  is defined as the average number of new infections caused by one infection in a population consisting of only susceptible hosts (Diekmann et al. 1990). In our case, we are working in units of C as opposed to host individuals, which changes the interpretation of  $R_0$  to some degree. To calculate  $R_0$ , we use the next-generation matrix (NGM) approach (Diekmann et al. 2010). In all cases, the pathogen can only invade the system if  $R_0$ 

> 1. Details and proofs are presented in the Supporting information.

## Model 1. A carbon-based logistic-growth model

We start with a logistic-growth model (Verhulst 1845, Pearl and Reed 1920), in which we track the density-dependent change in host biomass (*S*),

$$\frac{dS}{dt} = \rho_S \left( 1 - \theta_{bS} S \right) S - \delta_S \left( 1 + \theta_{mS} S \right) S \tag{1a}$$

which can be rewritten in the more traditional form of logistic growth

$$\frac{dS}{dt} = (\rho_S - \delta_S) \left( 1 - \frac{\rho_S \theta_{bS} + \delta_S \theta_{mS}}{\rho_S - \delta_S} S \right) S. \tag{1b}$$

In this model, change in total host biomass (S), measured in units of C, is determined by the balance of mass-specific death rate  $(\delta)$  and maximum mass-specific biomass production rate  $(\rho)$ , which can be considered as a maximum, mass-specific, C fixation (e.g. net primary productivity, NPP) rate for a primary producer. In other model formulations,  $(\rho_s - \delta_s)$  is represented as r, the intrinsic rate of population increase. This model includes linear density dependence of decreasing biomass production ( $\theta_{hs}$ ) and increasing death  $(\theta_{ms})$  rates, because this formulation allows us to isolate density dependent effects on host growth or death rates. Here  $\theta_{hS}$  and  $\theta_{mS}$  represent the strengths of density-dependence on growth and death rates, respectively. This negative density dependence could reflect a range of processes, including depletion of limiting resources (e.g. water, light, or elemental nutrients such as nitrogen or phosphorus), increasing pressure from natural enemies (e.g. herbivores, grazers), or physical crowding. However, these are not explicitly included in this model. Importantly, this density dependence allows for a finite, disease-free equilibrium, a characteristic necessary for the ecosystem model (model 3).

This model's solutions reach a stable, positive equilibrium,

$$S_1^* = \frac{\rho_S - \delta_S}{\rho_S \theta_{bS} + \delta_S \theta_{mS}} \tag{2}$$

when  $\rho_s > \delta_s$ . This expression  $\frac{\rho_S - \delta_S}{\rho_S \theta_{bS} + \delta_S \theta_{mS}}$  is functionally

analogous to the carrying capacity (K) of the canonical logistic growth model.

#### Model 2. A carbon-based disease model

We then extended our carbon-based logistic-growth model into a carbon-based, microparasite model with density-dependent transmission (SI model), which tracked the carbon (mass) in susceptible (S) and infected (I) hosts as well as carbon in the environmental pool of pathogens (P) (Fig. 1). In this model, we do not include a recovered class of hosts, as would be the case in a SIR model (Keeling and Rohani 2008). This model is based on a variety of canonical microparasite models (Anderson and May 1986, Keeling and Rohani 2008):

$$\frac{dS}{dt} = (\rho_S - \delta_S) \left( 1 - \frac{\rho_S \theta_{bS} + \delta_S \theta_{mS}}{\rho_S - \delta_S} (S + I) \right) S 
+ \rho_I \left( 1 - \theta_{bI} (S + I) \right) I - \beta SP$$
(3a)

$$\frac{dI}{dt} = \beta SP(1+\kappa) - \delta_I \left(1 + \theta_{mI} \left(S + I\right)\right) - b_I I \tag{3b}$$

$$\frac{dP}{dt} = b_I I - \kappa \beta SP - \delta_P P. \tag{3c}$$

In this model,  $\delta_i$  and  $\delta_i$  are the mass-specific death rates for susceptible and infected hosts respectively;  $\rho_{1}$  and  $\rho_{2}$  are the maximum mass-specific biomass production rates (i.e. NPP) for susceptible and infected hosts, respectively. β is the density-dependent transmission rate of the pathogen from the environmental pool of pathogens (P),  $b_{I}$  is the pathogen shedding rate from live infected hosts (I),  $\delta_p$  is the pathogen degradation rate in the environment, and  $\kappa$  represents the portion of the pathogen pool that is incorporated into the host during the infection process (e.g. the carbon in the spores or viral particles that enter the host during infection). As in model 1 (Eq. 1), we include the assumption of density-dependent effects on biomass production  $(\theta_{hS}, \theta_{hI})$  and death  $(\theta_{mS}, \theta_{mI})$  rates, which might differ for susceptible and infected hosts. Host biomass is finite in the absence of disease (e.g. in model 1 and 3), because of these assumptions of density-dependence.

Disease transmission is determined by the transmission rate of the pathogens ( $\beta$ ), the density of infected (I) and susceptible (S) host biomass, and the size of the pathogen pool (P), which depends on the density of infected host biomass (1) and the rate at which infected hosts shed pathogens into the environment. To link this model to ecosystem process rates, we frame this model in units of C (g C m<sup>-2</sup>), and our state variables (S, I and P) track the mass of C in host and pathogen biomass as opposed to numbers of individuals. While this approach is mathematically identical to the more familiar SI models, the biological interpretation is different, as C, is not infected but rather is contained within the mass of infected host individuals (Borer et al. 2021a). More specifically, we are tracking the total g of C that are contained within susceptible (S) or infected (I) hosts (Borer et al. 2021a), and the g of C that are contained within the pool of pathogens in the environment (P).

In the absence of a pathogen (I=0 and P=0), hosts will persist in the system if  $\rho_s > \delta_s$  with an equilibria density ( $S_1^*$ ; Eq. 2). While real, analytical solutions exist for the endemic equilibrium, the densities of susceptible hosts ( $S_2^*$ ), infected hosts ( $I_2^*$ ), and the environmental pathogen pool ( $I_2^*$ ) are too complex to present here.

The intrinsic rate of increase of the pathogen  $(R_0)$  is

$$R_0 = \frac{S_1^* \beta (1 + \kappa) b_I}{\left(\delta_I \left(1 + \theta_{mI} S_1^*\right) + b_I\right) \left(\kappa \beta S_1^* + \delta_P\right)}$$
(4a)

..or equivalently

$$R_0 = S_1^* \beta \left( 1 + \kappa \right) b_I \left( \frac{1}{\kappa \beta S_1^* + \delta_P} \right) \left( \frac{1}{\delta_I \left( 1 + \theta_{mI} S_1^* \right) + b_I} \right). \tag{4b}$$

In this second formulation (Eq. 4b),  $R_0$  can be decomposed into biologically relevant components, which all lead to increases in  $R_0$ : host density in the absence of disease ( $S_1^*$ ), transmission rate ( $\beta(1+\kappa)$ ), the shedding rate of the pathogen from infected hosts ( $b_I$ ), the duration of pathogen persistence in the environment  $\left(\frac{1}{\kappa\beta S_1^* + \delta_P}\right)$ , and infection

duration 
$$\left(\frac{1}{\delta_I \left(1 + \theta_{mI} S_1^*\right) + b_I}\right)$$
.

## Model 3. A carbon-based ecosystem model

As a complement to the carbon-based disease model (model 2), we developed an ecosystem model with no disease, in which we tracked the movement of C between three pools: live biomass (S), recently dead biomass or necromass ( $D_s$ , e.g. plant litter or suspended dead phytoplankton in the seston), and highly decomposed biomass or organic matter (W, e.g. soil organic matter or lake sediments; Fig. 1):

$$\frac{dS}{dt} = (\rho_S - \delta_S) \left( 1 - \frac{\rho_S \theta_{bS} + \delta_S \theta_{mS}}{\rho_S - \delta_S} (S + D_S) \right) S$$
 (5a)

$$\frac{dD_S}{dt} = \varepsilon \delta_S \left( 1 + \theta_{mS} \left( S + D_S \right) \right) S - \gamma_S D_S$$
 (5b)

$$\frac{dW}{dt} = \sigma \gamma_S D_S - \mu W. \tag{5c}$$

In addition to the parameters in model 1, we include the rate at which necromass (D) decomposes ( $\gamma$ ) and the rate at which organic matter (W) is lost to the system through processes such as leaching, erosion, or microbial respiration  $(\mu)$ . We account for losses of C (e.g. herbivory) by allowing only a fraction (E) of the dying biomass to be retained in the necromass pool and only a fraction of the decomposing necromass ( $\sigma$ ) to be retained in the organic matter pool (W). In this model, the host growth rate is limited by the accumulation of necromass (D) because of shading or the creation of a physical barrier (Shigesada and Okubo 1981, Bertness and Ellison 1987, Agustí 1991, Townsend et al. 1994, Foster and Gross 1998, Clark and Tilman 2010, Lønborg et al. 2013, Flynn and Raven 2017). Systems vary widely in the degree to which dead material limits host growth. This can be accounted for in this formulation by either reducing  $\varepsilon$  or increasing  $\gamma$ , which will reduce the accumulation of growthinhibiting dead material.

The nontrivial equilibrium for this model is:

$$S_{3}^{*} = \frac{\gamma_{S}(\rho_{S} - \delta_{S})}{(\varepsilon(\rho_{S}(\theta_{bS} + \theta_{mS})) + \gamma_{S}\theta_{mS})\delta_{S} + \gamma_{S}\rho_{S}\theta_{bS}}$$
(6)

$$D_{S3}^* = \frac{\varepsilon \delta_S \left( 1 + \theta_{mS} S_3^* \right) S_3^*}{\gamma_S - \varepsilon \delta_S \theta_{mS} S_3^*} \tag{7}$$

$$W_3^* = \frac{\sigma \gamma_S}{\mu} D_{S3}^* \tag{8}$$

This model includes negative density-dependent effects of necromass on host growth; however, decomposed organic material can eventually have a positive effect on plant growth, especially in terrestrial systems. For example, soil organic matter can mediate access to growth-limiting resources, such as water or soil nutrients, by increasing water-holding and cation-exchange capacity (Weil and Magdoff 2004). We explore the effects of including positive-density dependence of decomposed organic material (W) on host growth, which can potentially reduce the strength of the negative density dependence arising from recently dead material ( $D_S$ ), in the Supporting information.

## Model 4. A carbon-based disease-ecosystem model

Combining the disease and ecosystem models (model 2 and 3) is relatively straightforward, because we have framed them in units of C (Fig. 1). We separately track the abundance of necromass from susceptible  $(D_i)$  and infected  $(D_i)$  hosts, allowing us to incorporate environmental transmission of a pathogen as the shedding rate of the pathogen  $(b_D)$  from dead infected hosts (D<sub>1</sub>) (García-Guzmán and Benítez-Malvido 2003, Beckstead et al. 2012, Borer et al. 2021a). This also allows us to account for differential decomposition rates of infected  $(\gamma_i)$  and uninfected  $(\gamma_i)$  necromass (Omacini et al. 2004, Leroy et al. 2011, Grimmett et al. 2012, Cobb and Rizzo 2016, Pazianoto et al. 2019), which can arise through infection-induced changes in defensive compounds or tissue chemistry. This structure also allows for the case of partial infection, where infected tissue may be shed while the host remains living (e.g. a tree dropping an infected branch) or where an entire host dies but only a portion of the host tissue was infected.

This model is given by

$$\frac{dS}{dt} = (\rho_S - \delta_S) \left( 1 - \frac{\rho_S \theta_{bS} + \delta_S \theta_{mS}}{\rho_S - \delta_S} \left( S + I + D_S + D_I \right) \right) S$$

$$+ \rho_I \left( 1 - \theta_{bI} \left( S + I + D_S + D_I \right) \right) I - \beta SP$$
(9a)

$$\frac{dI}{dt} = \beta SP(1+\kappa) - \delta_I \left(1 + \theta_{mI} \left(S + I + D_S + D_I\right)\right) I - b_I I \quad (9b)$$

$$\frac{dD_S}{dt} = \varepsilon \delta_S \left( 1 + \theta_{mS} \left( S + I + D_S + D_I \right) \right) S - \gamma_S D_S \tag{9c}$$

$$\frac{dD_I}{dt} = \varepsilon \delta_I \left( 1 + \theta_{mI} \left( S + I + D_S + D_I \right) \right) I$$

$$-\gamma_I D_I - b_D D_I$$
(9d)

$$\frac{dP}{dt} = b_I I + b_D D_I - \kappa \beta SP - \delta_P P \tag{9e}$$

$$\frac{dW}{dt} = \sigma \gamma_S D_S + \sigma \gamma_I D_I - \mu W. \tag{9f}$$

In the absence of disease (I = 0, P = 0, and  $D_t = 0$ ), the nontrivial equilibria of this model are the same as in the ecosystem model (Eq. 6-8). Analytical solutions exist for the endemic equilibria density of susceptible hosts  $(S_4^*)$ , infected hosts  $(I_4^*)$ , infected and uninfected necromass  $(D_{S4}^*, D_{I4}^*)$ , the environmental pathogen pool  $(P_4^*)$ , and organic matter  $(W_4^*)$ ; however, they are too long and complex to be instructive, so we do not present them here.

The intrinsic rate of increase of the pathogen  $(R_0)$  is obtained by using the disease-free equilibrium:

$$R_{0} = \frac{S_{3}^{*}\beta(1+\kappa)((1+(S_{3}^{*}+D_{S1}^{*})\theta_{mI})\varepsilon b_{D}\delta_{I} + (b_{D}+\gamma_{I})b_{I}}{(b_{D}+\gamma_{I})(\kappa\beta S_{3}^{*}+\delta_{P})((1+(S_{3}^{*}+D_{S1}^{*})\theta_{mI})\delta_{I} + b_{I})}$$
(10a)

or equivalently

$$R_{0} = S_{3}^{*}\beta \left(1 + \kappa\right) \left(\frac{1}{\kappa \beta S_{1}^{*} + \delta_{P}}\right)$$

$$\begin{bmatrix} b_{I} \left(\frac{1}{\left(1 + \left(S_{3}^{*} + D_{S1}^{*}\right)\theta_{mI}\right)\delta_{I} + b_{I}}\right) \\ + b_{D} \left(\frac{1}{\gamma_{I} + b_{D}}\right) \left(\frac{\epsilon \delta_{I} \left(1 + \left(S_{1}^{*} + D_{S1}^{*}\right)\theta_{mI}\right)}{\left(1 + \left(S_{3}^{*} + D_{S1}^{*}\right)\theta_{mI}\right)\delta_{I} + b_{I}}\right) \end{bmatrix}. (10b)$$

While this equation is complex, the second formulation (Eq. 10b) reveals that  $R_0$  is composed of biologically meaningful components, which all serve to increase disease spread: host density in the absence of disease  $(S_3)$ , transmission rate  $(\beta(1+\kappa))$ , the duration of pathogen persistence in the environment  $\left(\frac{1}{\kappa\beta S_3^* + \delta_P}\right)$ , the transmission

pathway via live hosts  $b_I \left( \frac{1}{\left(1 + \left(S_3^* + D_{S3}^*\right)\theta_{mI}\right)\delta_I + b_I} \right)$ ,

and the transmission pathway via infected necromass

$$b_D \left(\frac{1}{\gamma_I + b_D}\right) \left(\frac{\varepsilon \delta_I \left(1 + \left(S_3^* + D_{S3}^*\right) \theta_{mI}\right)}{\left(1 + \left(S_3^* + D_{S3}^*\right) \theta_{mI}\right) \delta_I + b_I}\right). \text{ The live host}$$

transmission pathway can be decomposed into the shedding rate of the pathogen from infected hosts  $(b_i)$  and infection

duration of live hosts 
$$\left(\frac{1}{\left(1+\left(S_{3}^{*}+D_{S3}^{*}\right)\theta_{mI}\right)\delta_{I}+b_{I}}\right)$$
. The

infected necromass transmission pathway can be decomposed into the shedding rate of the pathogen from infected necromass

$$(b_D)$$
, infection duration of infected necromass  $\left(\frac{1}{\gamma_I + b_D}\right)$ ,

and proportion of the C from dying infected hosts that

becomes infected necromass 
$$\left(\frac{\varepsilon \delta_I \left(1 + \left(S_3^* + D_{S3}^*\right) \theta_{mI}\right)}{\left(1 + \left(S_3^* + D_{S3}^*\right) \theta_{mI}\right) \delta_I + b_I}\right).$$

Importantly, this model illustrates how disease spread rate is directly affected by C flux rates in the ecosystem, such as the decomposition rate  $(\gamma_t)$  and the loss of gaseous C from host biomass  $(1-\varepsilon)$  which can both reduce the amount necromass that can serve as a source of infection.

As with the Ecosystem model (model 3), we examine a model in which there is positive-density dependence of decomposed organic material (W) on host growth in the Supporting information.

## Model simplification to facilitate parameterization

All four models are written in terms of the effects of density-dependence on biomass production  $(\theta_{b}, \theta_{b})$  and death  $(\theta_{mS}, \theta_{mI})$  rates, which will vary for susceptible and infected hosts. To compare our models with empirical data, we make the following simplifying assumptions, which allow us to write the models in terms of a carrying capacity (K), a value we can estimate from readily available empirical data spanning a wide range of ecosystems and host vital rates. We start by assuming that density dependence acts only on biomass production rates ( $\theta_{mI} = \theta_{mS} = 0$ ) and that density dependence does not differ between susceptible and infected hosts ( $\theta_{bI} = \theta_{bS} = \alpha$ ). Under these assumptions, infection can still alter mass-specific death rates  $(\delta_s)$  $\neq \delta_{t}$ ) and the maximum mass-specific biomass production rates  $(\rho_s \neq \rho_t)$ , and all density-dependent effects are represented by a single parameter  $\alpha$ . We also assume that the portion of pathogen pool incorporated into the host during the infection process is vanishingly small ( $\kappa = 0$ ). Given these modifications, the full disease-ecosystem model (Eq. 9) can be rewritten as:

$$\frac{dS}{dt} = (\rho_S - \delta_S) \left( 1 - \frac{\rho_S \alpha}{\rho_S - \delta_S} (S + I + D_S + D_I) \right) S 
+ \rho_I \left( 1 - \alpha (S + I + D_S + D_I) \right) I - \beta SP$$
(11a)

$$\frac{dI}{dt} = \beta SP - \delta_I I - b_I I \tag{11b}$$

$$\frac{dD_S}{dt} = \varepsilon \delta_S S - \gamma_S D_S \tag{11c}$$

$$\frac{dD_I}{dt} = \varepsilon \delta_I I - \gamma_I D_I - b_D D_I \tag{11d}$$

$$\frac{dP}{dt} = b_I I + b_D D_I - \delta_P P \tag{11e}$$

$$\frac{dW}{dt} = \sigma \gamma_S D_S + \sigma \gamma_I D_I - \mu W. \tag{11f}$$

In the absence of disease (I=0, P=0 and  $D_I=0$ ), the non-trivial equilibrium of this model is

$$S_5^* = \frac{\gamma_S(\rho_S - \delta_S)}{\rho_S \alpha(\epsilon \delta_S + \gamma_S)}$$
 (12)

$$D_{S5}^* = \frac{\varepsilon \delta_S S_5^*}{\gamma_S} \tag{13}$$

$$W_5^* = \frac{\sigma \gamma_S}{u} D_{S5}^*. \tag{14}$$

Analytical solutions exist for the endemic equilibrial density of susceptible hosts  $(S_5^*)$ , infected hosts  $(I_5^*)$ , infected and uninfected necromass  $(D_{S5}^*, D_{I5}^*)$ , the environmental pool of pathogens  $(P_5^*)$ , and organic matter  $(W_5^*)$ ; however, they are too long and complex to present here. The intrinsic rate of increase of the pathogen  $(R_0)$  is

$$R_0 = \frac{S_5^* \beta \left( \varepsilon b_D \delta_I + b_I \left( b_D + \gamma_I \right) \right)}{\delta_P \left( b_D + \gamma_I \right) \left( \delta_I + b_I \right)}$$
(15a)

or equivalently

$$R_0 = S_5^* \beta \left(\frac{1}{\delta_P}\right) \left[ b_I \left(\frac{1}{\delta_I + b_I}\right) + b_D \left(\frac{1}{\gamma_I + b_D}\right) \left(\frac{\epsilon \delta_I}{\delta_I + b_I}\right) \right]. \quad (15b)$$

Under these simplifying assumptions,  $R_0$  depends on the same components as in the more complex model (Eq. 10b): host density in the absence of disease ( $S_5^*$ ), transmission rate ( $\beta$ ), the duration of pathogen persistence in the environment  $\left(\frac{1}{\delta_P}\right)$ , the transmission pathway via live hosts  $b_I\left(\frac{1}{\delta_I+b_I}\right)$ , and the transmission pathway via infected necromass  $b_D\left(\frac{1}{\gamma_I+b_D}\right)\left(\frac{\epsilon\delta_I}{\delta_I+b_I}\right)$ . As before, the live host transmission pathway can be decomposed into the shedding rate of

the pathogen from infected hosts  $(b_I)$  and infection duration of live hosts  $\left(\frac{1}{\delta_I + b_I}\right)$ . The infected necromass transmission pathway can be decomposed into the shedding rate of the pathogen from infected necromass  $(b_D)$ , the infection duration of infected necromass  $\left(\frac{1}{\gamma_I + b_D}\right)$ , and proportion of the C from dying infected hosts that becomes infected necromass  $\left(\frac{\epsilon \delta_I}{\delta_I + b_I}\right)$ . However, these components are markedly simpler than in the more complex disease–ecosystem model (Eq. 10). As in Eq. 10b, this reveals a direct link between disease persistence and key ecosystem rates, such as decomposition.

With these simplifying assumptions, Eq. 11a can then be rewritten as a function of K

$$\frac{dS}{dt} = (\rho_S - \delta_S) \left( 1 - \frac{S + I + D_S + D_I}{K} \right) S 
+ \rho_I \left( 1 - \alpha \left( S + I + D_S + D_I \right) \right) I - \beta SP$$
(16)

where

$$K = \frac{\rho_S - \delta_S}{\alpha \rho_S} \tag{17}$$

and

$$\alpha = \frac{\rho_S - \delta_S}{K \rho_S}.$$
 (18)

Equation 17 and 18 illustrate that the carrying capacity (K) represents a density-dependent scaling of the birth ( $\rho_S$ ) and death ( $\delta_S$ ) rates the strength of which is determined by the parameter ( $\alpha$ ).

Expressing transmission  $(\beta)$  in terms of prevalence (T) to facilitate parameterization

While our model includes transmission rates  $(\beta)$ , these are notoriously difficult to estimate in empirical systems and are rarely reported; however, transmission rates are closely related to disease prevalence, a much more empirically intuitive and measurable metric. We can solve for disease preva-

lence at equilibrium (T) as  $T = \frac{I^*}{I^* + S^*}$  and then express  $\beta$  as a function of T:

$$\beta(T) = \frac{A(((b_D + \gamma_I)\delta_S - \gamma_S\delta_I)\epsilon T - (\delta_S\epsilon + \gamma_S)(b_D + \gamma_I))\alpha}{((b_I + \delta_I - \delta_S - \rho_I + \rho_S)T - \rho_S + \delta_S)B}$$
(19)

where  $A=-(b_1+\delta_1)((\rho_1-\rho_S)T+\rho_S)\delta_P$  and  $B=\gamma_S(b_D\delta_1\epsilon+b_I(b_D+\gamma_I))$  (T-1). This function has two vertical asymptotes, the smaller of which provides a boundary for maximum prevalence at the endemic equilibrium. Prevalence increases as  $\beta$  increases, but as  $\beta$  continues to increase, prevalence will be

bounded by these asymptotes. One asymptote occurs when T = 1 (where 100% of hosts are infected) the second occurs when T satisfies the expression below:

$$T = \frac{\rho_S - \delta_S}{(\rho_S - \delta_S) - (\rho_I - \delta_I - b_I)}$$
$$= 1 + \frac{\rho_I - \delta_I - b_I}{(\rho_S - \delta_S) - (\rho_I - \delta_I - b_I)}$$
(20)

If  $\rho_S > \delta_S$  and  $\rho_I < \delta_I + b_I$ , the second asymptote is smaller than 1, and this value limits the maximum prevalence of the system. We use this to define the maximum prevalence at equilibrium (T) when  $\beta$  is sufficiently large:

$$T^* = min\left\{\frac{\rho_S - \delta_S}{(\rho_S - \delta_S) - (\rho_I - \delta_I - b_I)}, 1\right\}$$
(21)

which we can express in terms of intrinsic growth rates  $r_S = \rho_S$ -  $\delta_S$  and  $r_I = \rho_I - \delta_I - b_I$ 

$$T^* = min\left\{\frac{r_S}{r_S - r_I}, 1\right\}. \tag{22}$$

In this simpler formulation, the maximum prevalence at equilibrium (T) will be less than 1 when susceptible hosts have a positive population growth rate  $(r_S > 0)$  and the infected hosts do not  $(r_I < 0)$ . Finally, using this expression for T, we parameterized the value of  $\beta$  to yield half the maximum prev-

alence at endemic equilibrium, evaluating  $\beta\left(\frac{T^*}{2}\right)$  in Eq. 19.

## **Results**

## Insights from analytical solutions

The potential for a tight coupling between disease dynamics and ecosystem fluxes and pools is apparent from the analytical solutions of the integrated disease and ecosystem model (model 4) relative to the disease-only model (model 2) or the ecosystem-only model (model 3). This direct comparison is made possible by using C as currency, which can be tracked as it moves between living and nonliving states. While the integrated model (model 4) is more complex than either the disease (model 2) or ecosystem (model 3) models, it is unique in providing a single, integrated framework that can examine the interactive effects of disease (e.g. transmission and virulence) and ecosystem processes (e.g. primary productivity and decomposition) on state variables of relevance to both disease (e.g. prevalence and  $R_0$ ) and ecosystem ecology (e.g. live, dead, decomposed biomass).

The effects of ecosystem feedbacks on disease dynamics are apparent in the solutions for a pathogen's intrinsic rate of increase  $(R_0)$  in the integrated disease—ecosystem model (model 4) relative to the disease-only model (model 2).

As expected,  $R_0$  in both models depended on host density, pathogen transmission rates, and the death rate of infected hosts (Eq 4 and 10). However, the integrated disease-ecosystem model reveals disease-regulating mechanisms absent in the disease-only model. For example, by comparing model 2 and 3, dead host biomass (necromass) dynamics can alter a pathogen's intrinsic rate of increase  $R_0$  through two distinct pathways. First, dead biomass can serve as a source for the environmental reservoir of pathogens that infect susceptible hosts, thereby increasing  $R_0$ , in a process analogous to population-based disease models of systems with environmental pathogen pools (Breban et al. 2009, Fuller et al. 2012). Second, dead biomass can reduce the abundance of susceptible hosts, reducing  $R_0$  (Eq. 15). This second pathway is mediated by negative host density dependence. It is distinct from that found in typical models describing transmission from an environmental pool of pathogens, as it can alter  $R_0$  and host abundance even when dead biomass is not a source of pathogens ( $b_D = 0$ ). In the case where there are positive effects of decomposed organic matter on host growth (Supporting information), the suppressive effects of necromass may be reduced, thereby increasing disease spread. The strength of these effects is partly governed by decomposition rates, such that increased decomposition will reduce the suppressive effects of necromass on host growth while also reducing the source of infectious propagules. As a result, decomposition rates mediate the relationship between the rate of increase of pathogen  $(R_0)$  and transmission rate (Eq. 10b and 15b).

The pathways by which pathogens can alter elemental fluxes and pools are also apparent in the analytical solutions of the disease–ecosystem model (model 4) relative to the ecosystem model without disease (model 3). Most directly, pathogens can reduce C fixation via photosynthesis if  $\rho_S > \rho_I$  and increase the supply of dead host biomass to decomposers if  $\delta_I > \delta_S$  (Eq. 11). Pathogens also might alter decomposition, which controls the accumulation of necromass and organic matter if infected and uninfected cells or tissues decompose at different rates ( $\gamma_I \neq \gamma_S$ ). Finally, if necromass is a source of infection, this can reduce C fixation, highlighting a distinct pathway that becomes apparent only with the integration of disease and ecosystem models.

## Insights from model parameterization

In addition to the analytical solutions of these models, we examined model dynamics in biologically relevant parameter space by estimating parameter ranges and combinations that provide broad depictions of the dominant autotrophs found in four major terrestrial biomes (temperate grasslands, tropical forests, boreal forests, and temperate forests) and four major aquatic biomes (open oceans, coastal oceans, oligotrophic lakes, and eutrophic lakes) (Table 1, Supporting information). This more focused examination of biologically informed parameter values aimed to consider the model dynamics for reasonable parameter ranges and combinations, not to make quantitative predictions for specific biomes, conditions, or locations. Our estimates help build an intuition

for model dynamics in the regions of parameter space that capture a broad range of biologically informed values, rather than seeking to encompass the full range of potential parameters within biomes. Details on parameter estimation are presented in the Supporting information.

Using these parameters, we examined the effects of the transmission rate  $(\beta)$ , host density dependence  $\left(\alpha = \frac{\rho_S - \delta_S}{K \rho_S}\right)$ , and decomposition rates  $(\gamma = \gamma_I = \gamma_S)$  on  $R_0$ , maximum prevalence at equilibrium  $(T^*)$ , live biomass pools (S + I), and dead biomass pools  $(D_S + D_I)$ . Simulations reached stable equilibria for the model state variables for hosts with characteristics ranging from phytoplankton to trees (Supporting information).

Parameter values were highly correlated across the values estimated from the literature for the eight different biomes (Supporting information), suggesting that a lower dimensional representation of parameters could provide a summary of the model behavior. We used principal components analysis (PCA) to summarize the variation of five model parameters ( $\alpha$ ,  $\delta_s$ ,  $\rho_s$ ,  $b_\rho$ ,  $\gamma_s$ ); we excluded parameters derived from other parameters or state variables ( $\delta_p$ ,  $\rho_p$ ,  $b_D$ ,  $\gamma_p$ ,  $\beta_{BP}$ ) because of their inherent correlations. The first principal component (PC1) accounted for most of the total variance (77%) in parameter values. PC1 was characterized by the rate of host turnover, ranging from fast (aquatic phytoplankton) to slow (terrestrial vascular plants) (e.g.  $\delta_s$ ,  $\rho_s$  and  $\gamma_s$ ; Supporting information).

We used the system turnover rate (i.e. PC1) to gain general intuition for the disease (model 2), ecosystem (model 3), and ecosystem and disease (model 4) models, before examining

the effects of specific parameter combinations (Fig. 2). In most cases, all three models responded similarly to changes in system turnover rate (PC1). For example, live and dead host biomass pools declined with the system turnover rate, while prevalence increased with the system turnover rate. The general concordance among these models suggests that a carbon-based modeling framework can form the basis for a unified framework to link disease and ecosystem ecology.

While predictions were largely concordant, key differences among the models also became apparent. For example, the integrated ecosystem and disease model (model 4) predicted less live host biomass than the disease and ecosystem-only models (model 2 and 3), and this difference was largest in slow turnover systems (Fig. 2). The lower biomass in the disease–ecosystem model is likely due to necromass accumulation suppressing host growth combined with more pathogens being transmitted from dead hosts where decomposition rates were slow (Eq. 9; Supporting information). Because of the inclusion of necromass, the integrated disease–ecosystem model (model 4) also predicted higher prevalence and  $R_0$  in slow turnover systems and lower prevalence and  $R_0$  in fast turnover systems relative to the disease-only model (model 2).

We next examined the interactive effects of individual parameters on disease and host biomass while holding other parameters constant (Fig. 3, 4). As in our analyses using the single metric of host turnover rate (Fig. 2), the behavior of the integrated ecosystem and disease model (model 4) was broadly similar to the disease-only and ecosystem-only models (model 2 and 3) (Supporting information), suggesting that the C-based models can provide a coherent framework for integrating ecosystem and disease ecology.

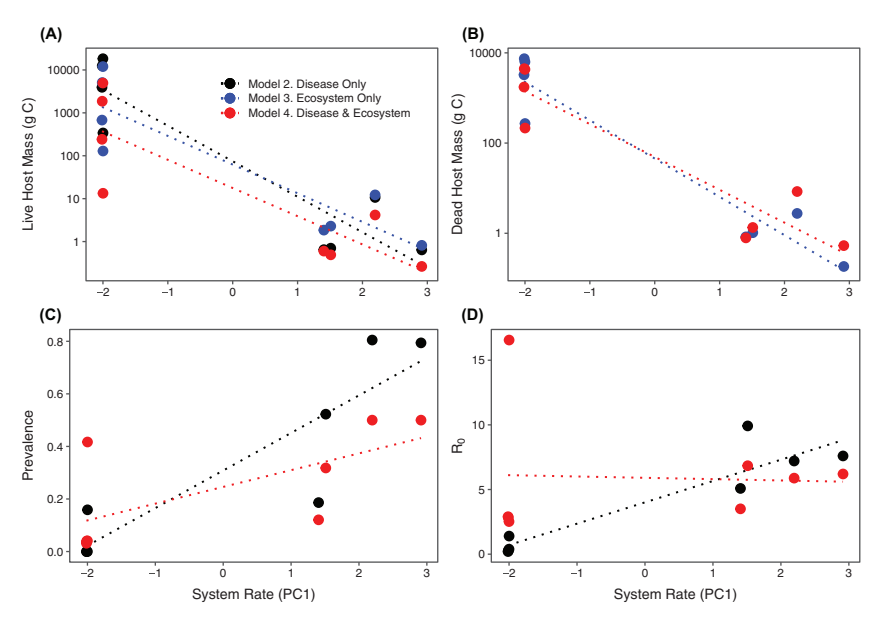


Figure 2. Comparison of disease model (model 2), ecosystem model (model 3), and disease and ecosystem model (model 4) predictions for (A) live biomass pools (S+I), (B) dead biomass pools  $(D_s+D_f)$  model 3 and 4 only), (C) pathogen prevalence at equilibrium ( $T^*$ ; model 2 and 4 only), and (D)  $R_0$  (model 2 and 4 only) along a gradient of system rate represented by the first principal component (PC1) of a PCA of the parameters in eight biomes (Supporting information). Higher values of PC1 represent faster turnover rates (e.g. growth, death and decomposition).

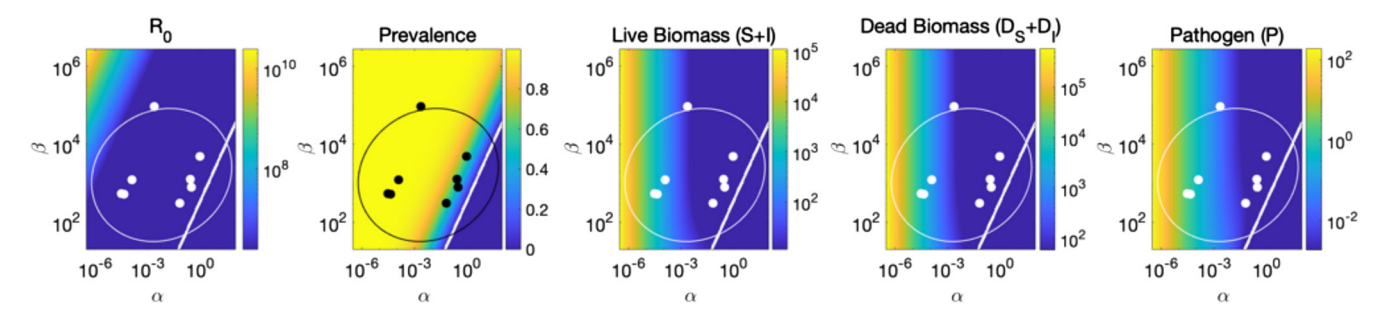


Figure 3. Effects of transmission rate ( $\beta$ ) and host density dependence ( $\alpha$ ) on  $R_0$ , prevalence at equilibrium  $T^*$ , live biomass pools (S+I) and dead biomass pools ( $D_S+D_I$ ). White line indicates the isocline above which disease can invade ( $R_0=1$ ). Points represent parameter values for the focal biomes and the ellipse represents the 90% confidence interval around these points. All other parameters are fixed at the average across ecosystems.

Disease invasion  $(R_0)$  and prevalence increased with the pathogen transmission rate ( $\beta$ ) and declined with the strength of host density dependence ( $\alpha$ ) (Fig. 3). This linkage between host density dependence and transmission is reflected in the positive slope of the disease invasion isocline  $(R_0 = 1)$ , which indicates that pathogen persistence requires higher transmission rates in systems with high levels of density dependence. These analyses also revealed the importance of ecosystem carbon fluxes in regulating disease dynamics. For example, disease invasion and prevalence increased with decomposition rates  $(\gamma_S, \gamma_I)$  for a given transmission rate (Fig. 4). The importance of decomposition rate also is reflected in the disease invasion isocline, which shows that lower transmission rates are needed for the disease to invade when decomposition rates are high (Fig. 4). The overall positive effect of decomposition on disease suggests that suppression of host growth by dead biomass had stronger effects on disease dynamics than the increased supply of pathogens from necromass. This insight arises only from simultaneously considering disease and ecosystem dynamics.

The pools of live and dead host biomass were controlled by interactions between host density dependence ( $\alpha$ ), decomposition rate ( $\gamma_S$ ,  $\gamma_I$ ), and pathogen transmission rate ( $\beta$ ) (Fig. 3, 4). Host density dependence reduced live and dead biomass, regardless of the pathogen transmission rate. In contrast, decomposition rate and pathogen transmission strongly

interacted to control the accumulation of live and dead host biomass. Peak live biomass occurred when the transmission rate was low and decomposition was high, while the highest levels of dead biomass occurred at low decomposition and transmission rates (Fig. 4). This interaction also was manifested in the effects of decomposition on the disease invasion isocline; the decomposition rate determines a threshold below which the disease cannot invade. As a result, the model predicts that only highly transmissible pathogens can invade systems with low decomposition rates.

## Discussion

Disease and ecosystem ecology have remained disparate disciplines due to their different conceptual lineages. Our modeling framework builds from recent work revealing the complementarity of these fields and the prospects for novel insights arising from tighter integration (Preston et al. 2016, Borer et al. 2021a, 2022). A key to this integration is working in units of elements (here, C), a currency that can be tracked between healthy and infected host states, as well as between living and non-living states (Borer et al. 2021a, 2022) and environmental pools of pathogens, themselves. In our analyses, the behavior of the integrated disease and ecosystem model (model 4) was broadly similar to our versions of

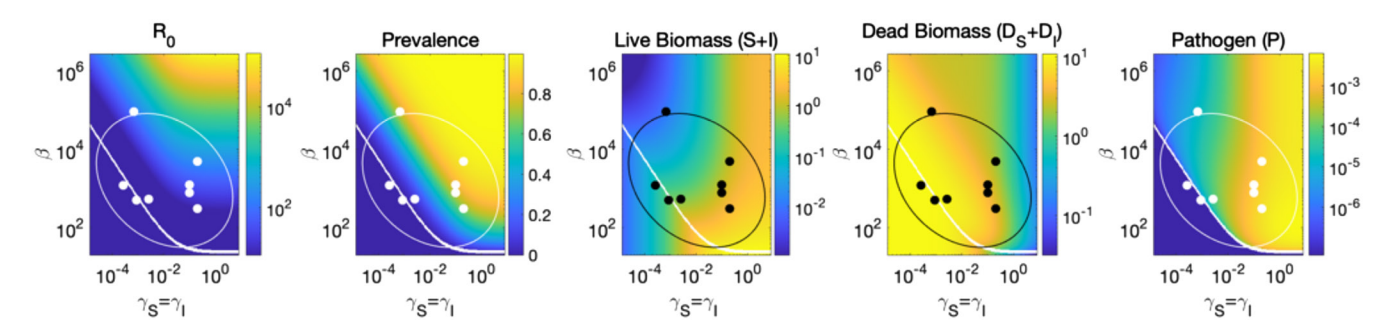


Figure 4. Effects of transmission rate ( $\beta$ ) and decomposition rate ( $\gamma = \gamma_I = \gamma_S$ ) on  $R_0$ , maximum prevalence at equilibrium ( $T^*$ ), live biomass pools (S + I) and dead biomass pools ( $D_S + D_I$ ). White line indicates the isocline above which disease can invade ( $R_0 = 1$ ). Points represent parameter values for the focal biomes and the ellipse represents the 90% confidence interval around these points. All other parameters are fixed at the average across ecosystems.

canonical disease-only and ecosystem-only models (model 2 and 3) (Supporting information), suggesting that the C-based models can provide a coherent framework for integrating well-developed theory in ecosystem and disease ecology.

This integrated framework builds on other recent work exploring the feedbacks between disease and ecosystem dynamics within a single model framed around elemental fluxes (Borer et al. 2021a, 2022). Taken together this theoretical work suggests that ecosystem—disease feedbacks are likely to be generally important. The models presented here simplify earlier work by focusing solely on carbon dynamic fluxes, which has several advantages. The carbon-based models have many fewer parameters than stoichiometric models (Borer et al. 2021a, 2022), which are more readily estimable in empirical systems. The carbon-based models are also more tractable analytically, having closed-form analytical solutions independent of empirical parameters.

Our analytical and simulation-based analyses of these models demonstrate that ecosystem processes, such as decomposition, can strongly affect host—pathogen interactions and that disease can fundamentally alter the cycling rates and pools of elements. Despite the logical evidence of the importance of the disease—ecosystem feedbacks, these are rarely explored experimentally, and disease is rarely considered in ecosystem ecology.

A comparison of the C-based, disease-ecosystem model (model 4) with the disease (model 2) or ecosystem (model 3) models reveals new dynamics that emerge when we explicitly link disease and ecosystem ecology. For example, accounting for dead host biomass altered host-pathogen dynamics in several ways, including the direct transmission of pathogens from dead hosts (García-Guzmán and Benítez-Malvido 2003, Beckstead et al. 2012, Borer et al. 2021a) and density-dependent suppression of host growth by dead host biomass (Agustí 1991, Foster and Gross 1998, Clark and Tilman 2010, Lønborg et al. 2013). As a result, the decomposition rate of dead hosts was integral to pathogen spread  $(R_0)$ , because decomposition regulated dead host biomass accumulation. While some existing disease ecology models include environmental transmission (Breban et al. 2009, Fuller et al. 2012), the direct suppression of host growth by dead host biomass remains largely unexplored in disease ecology. Although the theoretical results presented here suggest a strong co-regulation of pathogens, disease, and elemental cycling, there have been very few experiments mechanistically examining these linkages.

In the integrated disease–ecosystem model, pathogens altered important ecosystem fluxes and the size of C pools of live biomass, dead biomass (e.g. litter or phytoplankton), and decomposed organic C (e.g. soil or lake and ocean sediments). These pathogen effects arose through several routes. First, infected hosts could experience reduced C fixation rates (i.e. photosynthesis) (Suttle et al. 1990, Kohli et al. 2021), which reduced the C supply to the whole ecosystem (Seabloom et al. 2017, Cappelli et al. 2020). Second, infection could increase host death rates, thereby increasing the supply of dead biomass to decomposers and ultimately the

influx of C to the longer-term C pools in soils or sediments (Jiao et al. 2010, Cobb et al. 2012, Weitz and Wilhelm 2012, Preston et al. 2016, Borer et al. 2021a). Finally, infected and uninfected necromass could decompose at different rates, controlling the size of the dead biomass pool (Omacini et al. 2004, Jiao et al. 2010, Leroy et al. 2011, Grimmett et al. 2012, Weitz and Wilhelm 2012, Cobb and Rizzo 2016, Pazianoto et al. 2019, Borer et al. 2021a).

The current modeling exercise aims to maintain generality by generating analytical solutions while also exploring model dynamics across a broad array of biologically relevant parameter values. While we examine model dynamics in the parameter space describing terrestrial, marine, and freshwater biomes, our intention is not to provide an accurate model for any specific system. Instead, these parameter combinations allowed us to visualize the model dynamics for different, biologically motivated regions of parameter space. This examination of dynamics across a wide range of parameter combinations arising from many biomes revealed that the largest dynamical differences were between parameters estimated from aquatic and terrestrial biomes, reflecting a fastslow parameter value continuum (Wright et al. 2004, Reich 2014, Bonetti et al. 2019). Interestingly, the models predict that disease effects will increase with host turnover rates; the models predicted much higher prevalence in fast turnover systems (e.g. aquatic ecosystems). This result is concordant with the observation that viruses have been estimated to kill 20% of all marine microbial biomass each day (Fuhrman 1999, Suttle 2005, Suttle 2007), a mortality rate that far exceeds anything that has been documented in slower turnover ecosystems (e.g. forests). The prediction of higher disease impacts in fast turnover biomes also may apply within systems. Cappelli et al. (2020) found fungal pathogens had the largest effects on biomass in experimental grasslands dominated by fast-growing plant species.

The results spanning wide ranges of parameter values suggest the potential for novel questions, hypotheses, and insights arising from theory that integrates disease and ecosystem ecology. For example, they highlight the importance of decomposition rates in driving new production, thereby, enabling higher transmission rates and prevalence of infection. We are not aware of any direct empirical tests of whether the presence of pathogens alters the relationship between live and dead biomass or whether these effects are altered by decomposition rates. At global scales, there are only weak correlations between live and dead biomass in terrestrial grasslands (O'Halloran et al. 2013), a pattern that more closely mirrors the predictions of the integrated disease-ecosystem model (model 4) compared to the ecosystem model (model 3, that predicts a closer coupling of live and dead biomass) (Supporting information).

Recycling of elements is a core component of many ecosystem models (Lindeman 1942, Morowitz 1968, Ulanowicz 1972, Harwell et al. 1977) that is not included in the current model formulation, though it has been addressed elsewhere (Borer et al. 2022). The critical effect of disease on nutrient recycling is well illustrated in marine systems, where viral

lysis of microbial hosts can increase organic matter recycling and net primary productivity (i.e., the viral shunt; Wilhelm and Suttle 1999, Weitz et al. 2015).

Feedbacks arising from elemental recycling might only emerge in terrestrial systems over long periods of time. For example, C from decomposing litter can increase soil fertility by increasing the availability of growth-limiting resources, such as water or soil nutrients. This in turn can increase water-holding and cation-exchange capacity (Weil and Magdoff 2004) and thereby increase plant (host) productivity (Isbell et al. 2019, Seabloom et al. 2021). While our model only includes negative density effects of recently dead hosts, effects of positive feedbacks can be seen in the model variation in which accumulation of decomposed organic matter can increase host growth rates (Supporting information), thereby increasing host biomass in the absence of disease and increasing disease spread ( $R_0$ ).

However, fully addressing these types of feedbacks requires stoichiometric models that explicitly include growth-limiting nutrients, such as nitrogen or phosphorus. Recent models of this sort have demonstrated that nutrient recycling in disease systems is highly destabilizing. However, the destabilizing effects depend partly on the pathogen impacts on host demography (Borer et al. 2022). A challenge for future modeling of elemental recycling is the vastly different time scales that govern host-pathogen dynamics (e.g. photosynthesis and disease transmission) and longer time scales of biogeochemical feedbacks that affect hosts' vital rates, such as soil development or lake turnover (Knops and Tilman 2000, Bonetti et al. 2019). Despite these challenges, theoretical investigations, and empirical tests of the effects of elemental recycling represent an essential frontier with both basic and applied importance.

Infection of primary producers by pathogens might change the elemental and biochemical composition of host tissue with consequences for the decomposition rate of dead host biomass. Although we did not explore the dynamical consequences here, recent work has generated a modeling framework using a stoichiometric approach to examine disease-ecosystem interactions (Borer et al. 2021a, 2022). Changes in host stoichiometry and their consequences for elemental cycling are attributed to the impact pathogens might have on host metabolism (i.e. photosynthetic activity, growth, and development), as well as by inducing host defense mechanisms (Berger et al. 2007, Bolton 2009), which might alter the rate of decomposition. Microbes can trigger increased metabolic rates of hosts by hijacking plant carbohydrate and nutrient metabolism (Bolton 2009, Fagard et al. 2014, Oliva et al. 2014, Rojas et al. 2014, Schwachtje et al. 2018), and altering plant nutrient content, which can impact decomposition rates (Wolfe and Ballhorn 2020). For example, activation of host defenses against pathogens via secondary metabolites can upregulate host nitrogen uptake and mobilization (Mur et al. 2017), and some endophytic fungi (e.g. Rhytisma acerinum) and bacteria can inhibit or enhance N or P reabsorption before leaf senescence. Both of these processes can impact litter nutrient content (Cornelissen et al. 2000,

Cao et al. 2015), which can, in turn, control organic matter decomposition and the rate of carbon cycling (Aerts 1997). The production of defensive phenolic compounds (e.g. tannins) also affects decomposition rates by forming polyphenol-protein complexes (Hattenschwiler and Vitousek 2000) that are resistant to the breakdown by most microorganisms (Hattenschwiler and Vitousek 2000, Ormeno et al. 2006, Chomel et al. 2014, Chomel et al. 2016). Modeling has demonstrated that linking carbon and nutrient content of hosts can alter predictions for infectious disease (Borer et al. 2021a), but this stoichiometric approach has significant challenges for finding analytical solutions and has, to date, relied on simulations across finite parameter ranges. Nonetheless, these pervasive feedbacks between metabolic or defensive compounds, infection, and carbon cycling suggest that this is a fruitful area for future work.

Despite empirical and theoretical evidence for dynamically meaningful linkages between disease and elemental cycles, there are few experimental studies that concurrently manipulate pathogens and measure elemental fluxes. Nevertheless, this type of experiment would provide the strongest tests of this theory and the best opportunity for data model integration. An example of the type of work that is needed is a long-term fungicide experiment conducted in both natural and experimental grasslands in the tallgrass prairie ecosystem of central North America (Borer et al. 2015, Seabloom et al. 2017, Kohli et al. 2019, Kohli et al. 2021). This experiment demonstrated that reducing foliar fungal pathogens increased mass-specific C fixation  $(\rho S + \rho I)$  leading to significantly higher pools of live biomass (S+I) (Seabloom et al. 2017, Kohli et al. 2019, Kohli et al. 2021). These results validate core assumptions of the model structure, such as assuming mass-specific effects of pathogens on C fixation.

Some of the effects of pathogen reduction on C fluxes in grasslands are mediated by changes in plant tissue chemistry (Borer et al. 2015, Kohli et al. 2019). Two fungicide studies have demonstrated that applications of foliar fungicides increase the dominance of fast-growing plants with high levels of tissue N. These linkages suggest that a stoichiometric approach might yield additional insights (Borer et al. 2021a, b). In addition, these studies demonstrate that the effects of pathogens on nutrient cycling will be impacted by changes in community composition (Cappelli et al. 2020, Kohli et al. 2021), suggesting critical knowledge gaps at the nexus of the community and ecosystem ecology of disease. As we seek to understand better both the role of disease and the fluxes of carbon and other elements in natural systems, these system-specific experimental results and the general theoretical results presented here highlight the importance of additional experimental tests of the role of pathogens in mediating elemental fluxes.

While we have focused on autotrophic hosts (e.g. plants and phytoplankton), this work also might be informative of dynamics of heterotrophic hosts. For example, in many systems dead hosts play key roles in serving as environmental reservoirs for animal pathogens (Hampson et al. 2011, Fuller et al. 2012, Miller et al. 2014, Escobar et al. 2020). In

prion diseases, such as chronic wasting disease (CWD), infectious prions can remain in the environment, shed from decomposed carcasses, for years (Miller et al. 2014, Escobar et al. 2020). Similarly, the transmission of anthrax Bacillus anthracis among herbivore hosts largely depends on indirect exposure to spores released from carcasses (Hampson et al. 2011). Despite the potential risk of anthrax exposure, there is some evidence suggesting that carcass-mediated nutrient pulses could attract herbivores (Turner et al. 2014), pointing to the intriguing idea that feedbacks between host death and transmission risk could be mediated by nutrient cycling across trophic levels. How mobile hosts might behaviorally mediate their risk to such potential exposures is a separate question not captured in our modeling framework. The current work suggests that examining such host-parasite feedbacks is an open and important future direction to consider (Ezenwa et al. 2016).

Working in a currency of elements allows us to link canonical disease and ecosystem models (Borer et al. 2021a); however, the current model does not nest carbon within individual hosts. In contrast, most disease models assume that entire hosts become infected instantaneously (Keeling and Rohani 2008). This whole-host infection approach does not capture dynamics such as the abscission of infected tissues or whole leaves but the retention of uninfected tissue. Some models in disease ecology use a hierarchical structure whereby infection proceeds through a host and then spreads from host to host (Borer et al. 2016, Strauss et al. 2019). A possible extension of the current model could be to incorporate this hierarchical approach, recognizing that infected biomass occurs within a host individual, and infection spread through host tissues will likely proceed at very different rates than transmission among hosts (Borer et al. 2016). This approach also could allow explicit incorporation of host body size, which can be an important determinant of disease dynamics (Kuris et al. 1980, George-Nascimento et al. 2004, Seabloom et al. 2015, Borer et al. 2022) and differs widely among ecosystems. For example, in the current model, host differences among biomes are reflected in C turnover rates (e.g. photosynthesis and death rates); however, the spread of a pathogen through a single tree (with many differentiated cells) differs substantially from the spread through a population of single phytoplankton cells. While we expect that these more complex models will not be as analytically tractable as those presented here (Strauss et al. 2019), a hierarchical approach would, nonetheless, open many new areas of

Despite their disparate lineages and conceptual frameworks, disease and ecosystem ecology share a recognition of the importance of microbes in regulating critical rates in their respective disciplines. In disease ecology, microbial pathogens regulate the movement of material from biotic to abiotic pools via host death. Conversely, in ecosystem models, microbes regulate the conversion of dead material into biologically accessible sources of energy and matter (e.g. via decomposition). However, these differing approaches lead to conceptual gaps. For example, while ecosystem ecology has

recognized the primacy of microbes in regulating the breakdown of organic C (e.g. microbial respiration and decomposition), the field has given little attention to the impacts of microbes on C fixation through altered carbon fixation rates (but see, Kohli et al. 2021). În addition, the important role of pathogens in determining the supply of organic carbon to the decomposer food web has received little attention (Cobb et al. 2012). In a scan of ecosystem ecology textbooks, we found no references to disease or pathogens (Chapin et al. 2002, Schlesinger and Bernhardt 2013). In addition, there have been very few experiments that specifically examine the effects of pathogens on ecosystem processes. Given the appreciation for the importance of microbes in ecosystem ecology, we expect that integrating microbial pathogens into this field will be a natural extension (Preston et al. 2016, Borer et al. 2021a). More broadly, we expect that a unified framework for ecosystem and disease ecology can move both fields forward, yielding exciting conceptual advances and providing a foundation for empirical hypothesis testing.

Acknowledgements – Funding – This work was supported by a grant to ETB from the Natl Socio-Environmental Synthesis Center (SESYNC) under funding received from the Natl Science Foundation DBI-1639145. This work was supported by grants from the US Natl Science Foundation Long-Term Ecological Research Program (LTER) including DEB-1831944.

#### **Author contributions**

Eric W. Seabloom: Conceptualization (lead); Formal analysis (supporting); Funding acquisition (equal); Investigation (equal); Project administration (equal); Writing – original draft (lead). Angela Peace: Conceptualization (supporting); Formal analysis (equal); Investigation (equal); Writing - review and editing (equal). Lale Asik: Conceptualization (supporting); Formal analysis (equal); Investigation (equal); Writing – review and editing (equal). Rebecca Everett: Conceptualization (supporting); Formal analysis (equal); Investigation (equal); Writing - review and editing (equal). **Thijs Frenken**: Conceptualization (supporting); Investigation (equal); Writing - review and editing (equal). Angélica L. Gonzalez: Conceptualization (supporting); Investigation (equal); Writing – original draft (equal). **Alex T. Strauss:** Conceptualization (supporting); Formal analysis (supporting); Investigation (equal); Writing - review and editing (equal). Dedmer B. Van de Waal: Conceptualization (supporting); Investigation (equal); Writing - review and editing (equal). Lauren A. White: Conceptualization (supporting); Formal analysis (supporting); Investigation (equal); Writing - review and editing (equal). Elizabeth T. Borer: Conceptualization (equal); Funding acquisition (equal); Investigation (equal); Project administration (equal); Writing - review and editing (equal).

#### Data availability statement

Data sharing is not applicable to this article as no new data were created or analyzed in this study.

## **Supporting information**

The Supporting information associated with this article is available with the online version.

## References

- Aerts, R. 1997. Climate, leaf litter chemistry and leaf litter decomposition in terrestrial ecosystems: a triangular relationship. Oikos 79: 439–449.
- Agustí, S. 1991. Light environment within dense algal populations: cell size influences on self-shading. J. Plankton Res. 13: 863–871.
- Anderson, R. M. and May, R. M. 1986. The invasion, persistence and spread of infectious diseases within animal and plant communities. – Phil. Trans. R. Soc. B 314: 533–570.
- Bar-On, Y. M., Phillips, R. and Milo, R. 2018. The biomass distribution on Earth. Proc. Natl Acad. Sci. USA 115: 6506–6511.
- Beckstead, J., Miller, L. E. and Connolly, B. M. 2012. Direct and indirect effects of plant litter on a seed–pathogen interaction in *Bromus tectorum* seed banks. Seed Sci. Res. 22: 135–144.
- Berger, S., Sinha, A. K. and Roitsch, T. 2007. Plant physiology meets phytopathology: plant primary metabolism and plant-pathogen interactions. J. Exp. Bot. 58: 4019–4026.
- Bertness, M. D. and Ellison, A. M. 1987. Determinants of pattern in a new-england salt-marsh plant community. Ecol. Monogr. 57: 129–147.
- Bolton, M. D. 2009. Primary metabolism and plant defense-fuel for the fire. Mol. Plant-Microbe Interact. 22: 487–497.
- Bonetti, G., Trevathan-Tackett, S. M., Carnell, P. E. and Macreadie,
  P. I. 2019. Implication of viral infections for greenhouse gas dynamics in freshwater wetlands: challenges and perspectives.
  Front. Microbiol. 10: 1962.
- Borer, E. T., Lind, E. M., Ogdahl, E. J., Seabloom, E. W., Tilman, D., Montgomery, R. A. and Kinkel, L. L. 2015. Food-web composition and plant diversity control foliar nutrient content and stoichiometry. – J. Ecol. 103: 1432–1441.
- Borer, E. T., Laine, A. L. and Seabloom, E. W. 2016. A multiscale approach to plant disease using the metacommunity concept. Annu. Rev. Phytopathol.54: 397–418.
- Borer, E. T., Asik, L., Everett, R. A., Frenken, T., Gonzalez, A. L.,
  Paseka, R. E., Peace, A., Seabloom, E. W., Strauss, A. T., Van de Waal, D. B. and White, L. A. 2021a. Elements of disease in a changing world: modelling feedbacks between infectious disease and ecosystems. Ecol. Lett. 24: 6–19.
- Borer, E. T. et al. 2021b. Nutrients cause grassland biomass to outpace herbivory. Nat. Commun. 12: 6036.
- Borer, E. T., Paseka, R. E., Peace, A., Asik, L., Everett, R., Frenken, T., Gonzalez, A. L., Strauss, A. T., Van de Waal, D. B., White, L. A. and Seabloom, E. W. 2022. Disease-mediated nutrient dynamics: coupling host–pathogen interactions with ecosystem elements and energy. Ecol. Monogr. 92: e1510.
- Breban, R., Drake, J. M., Stallknecht, D. E. and Rohani, P. 2009. The role of environmental transmission in recurrent avian influenza epidemics. – PLoS Comput. Biol. 5: 11.
- Brewer, J. S., Levine, J. M. and Bertness, M. D. 1998. Interactive effects of elevation and burial with wrack on plant community structure in some Rhode Island salt marshes. J. Ecol. 86: 125–136.
- Brookes, V. J., Durr, S. and Ward, M. P. 2019. Rabies-induced behavioural changes are key to rabies persistence in dog populations: investigation using a network-based model. PLoS Neglected Trop. Dis. 13: 19.

- Cao, J. R., Cheng, C. Z., Yang, J. J. and Wang, Q. B. 2015. Pathogen infection drives patterns of nutrient resorption in citrus plants. Sci. Rep. 5: 14675.
- Cappelli, S. L., Pichon, N. A., Kempel, A. and Allan, E. 2020. Sick plants in grassland communities: a growth-defense tradeoff is the main driver of fungal pathogen abundance. Ecol. Lett. 23: 1349–1359.
- Chapin, F. S., Matson, P. A. Mooney, H. A. and Vitousek, P. M. 2002. Principles of terrestrial ecosystem ecology. Springer.
- Chapin, F. S., Matson, P. A. and Vitousek, 2012. Principles of terrestrial ecosystem ecology, 2nd edn. Springer.
- Chomel, M., Fernandez, C., Bousquet-Melou, A., Gers, C., Monnier, Y., Santonja, M., Gauquelin, T., Gros, R., Lecareux, C. and Baldy, V. 2014. Secondary metabolites of Pinus halepensis alter decomposer organisms and litter decomposition during afforestation of abandoned agricultural zones. J. Ecol. 102: 411–424.
- Chomel, M., Guittonny-Larcheveque, M., Fernandez, C., Gallet, C., DesRochers, A., Pare, D., Jackson, B. G. and Baldy, V. 2016. Plant secondary metabolites: a key driver of litter decomposition and soil nutrient cycling. J. Ecol. 104: 1527–1541.
- Clark, C. M. and Tilman, D. 2010. Recovery of plant diversity following N cessation: effects of recruitment, litter, and elevated N cycling. Ecology 91: 3620–3630.
- Cobb, R. C. and Rizzo, D. M. 2016. Litter chemistry, community shift, and non-additive effects drive litter decomposition changes following invasion by a generalist pathogen. Ecosystems 19: 1478–1490.
- Cobb, R. C., Chan, M. N., Meentemeyer, R. K. and Rizzo, D. M. 2012. Common factors drive disease and coarse woody debris dynamics in forests impacted by sudden oak death. – Ecosystems 15: 242–255.
- Cobb, R. C., Eviner, V. T. and Rizzo, D. M. 2013. Mortality and community changes drive sudden oak death impacts on litterfall and soil nitrogen cycling. New Phytol. 200: 422–431.
- Cornelissen, J. H. C., Perez-Harguindeguy, N., Gwynn-Jones, D., Diaz, S., Callaghan, T. V. and Aerts, R. 2000. Autumn leaf colours as indicators of decomposition rate in sycamore (*Acer pseudoplatanus* L.). Plant Soil 225: 33–38.
- Diekmann, O., Heesterbeek, J. A. P. and Metz, J. A. J. 1990. On the definition and the computation of the basic reproduction ratio R0 in models for infectious diseases in heterogeneous populations. J. Math. Biol. 28: 365–382.
- Diekmann, O., Heesterbeek, J. A. P. and Roberts, M. G. 2010. The construction of next-generation matrices for compartmental epidemic models. J. R. Soc. Interface 7: 873–885.
- Escobar, L. E., Pritzkow, S., Winter, S. N., Grear, D. A., Kirchgessner, M. S., Dominguez-Villegas, E., Machado, G., Peterson, A. T. and Soto, C. 2020. The ecology of chronic wasting disease in wildlife. Biol. Rev. 95: 393–408.
- Ezenwa, V. O., Archie, E. A., Craft, M. E., Hawley, D. M., Martin, L. B., Moore, J. and White, L. 2016. Host behaviour–parasite feedback: an essential link between animal behaviour and disease ecology. Proc. R. Soc. B 283: 20153078.
- Fagard, M., Launay, A., Clement, G., Courtial, J., Dellagi, A., Far-jad, M., Krapp, A., Soulie, M. C. and Masclaux-Daubresse, C. 2014. Nitrogen metabolism meets phytopathology. J. Exp. Bot. 65: 5643–5656.
- Fischhoff, I. R., Huang, T., Hamilton, S. K., Han, B. A., LaDeau, S. L., Ostfeld, R. S., Rosi, E. J. and Solomon, C. T. 2020. Parasite and pathogen effects on ecosystem processes: a quantitative review. Ecosphere 11: e03057.
- Flynn, K. J. and Raven, J. A. 2017. What is the limit for photoautotrophic plankton growth rates? J. Plankton Res. 39: 13–22.

- Foster, B. L. and Gross, K. L. 1998. Species richness in a successional grassland: effects of nitrogen enrichment and plant litter. Ecology 79: 2593–2602.
- Fuhrman, J. A. 1999. Marine viruses and their biogeochemical and ecological effects. Nature 399: 541–548.
- Fuller, E., Elderd, B. D. and Dwyer, G. 2012. Pathogen persistence in the environment and insect–baculovirus interactions: disease-density thresholds, epidemic burnout, and insect outbreaks. Am. Nat. 179: E70–E96.
- García-Guzmán, G. and Benítez-Malvido, J. 2003. Effect of litter on the incidence of leaf-fungal pathogens and herbivory in seedlings of the tropical tree *Nectandra ambigens*. – J. Trop. Ecol. 19: 171–177.
- George-Nascimento, M., Munoz, G., Marquet, P. A. and Poulin, R. 2004. Testing the energetic equivalence rule with helminth endoparasites of vertebrates. Ecol. Lett. 7: 527–531.
- Grimmett, I. J., Smith, K. A. and Barlocher, F. 2012. Tar-spot infection delays fungal colonization and decomposition of maple leaves. – Freshwater Sci. 31: 1088–1095.
- Hampson, K., Lembo, T., Bessell, P., Auty, H., Packer, C., Halliday,
  J., Beesley, C. A., Fyumagwa, R., Hoare, R., Ernest, E., Mentzel,
  C., Metzger, K. L., Mlengeya, T., Stamey, K., Roberts, K., Wilkins,
  P. P. and Cleaveland, S. 2011. Predictability of anthrax infection
  in the Serengeti, Tanzania. J. Appl. Ecol. 48: 1333–1344.
- Harwell, M. A., Cropper, W. P. and Ragsdale, H. L. 1977. Nutrient recycling and stability re-evaluation. Ecology 58: 660–666.
- Hattenschwiler, S. and Vitousek, P. M. 2000. The role of polyphenols in terrestrial ecosystem nutrient cycling. Trends Ecol. Evol. 15: 238–243.
- Heesterbeek, J. A. P. and Roberts, M. G. 2015. How mathematical epidemiology became a field of biology: a commentary on Anderson and May (1981) 'The population dynamics of microparasites and their invertebrate hosts'. Phil. Trans. R. Soc. B 370: 20140307.
- Holt, R. D. and Pickering, J. 1985. Infectious disease and species coexistence: a model of Lotka–Volterra form. – Am. Nat. 126: 196–211.
- Isbell, F., Tilman, D., Reich, P. B. and Clark, A. T. 2019. Deficits of biodiversity and productivity linger a century after agricultural abandonment. – Nat. Ecol. Evol. 3: 1533–1538.
- Jacquet, S., Miki, T., Noble, R., Peduzzi, P. and Wilhelm, S. 2010. Viruses in aquatic ecosystems: important advancements of the last 20 years and prospects for the future in the field of microbial oceanography and limnology. – Adv. Oceanogr. Limnol. 1: 97–141.
- Jiao, N., Herndl, G. J., Hansell, D. A., Benner, R., Kattner, G., Wilhelm, S. W., Kirchman, D. L., Weinbauer, M. G., Luo, T. W., Chen, F. and Azam, F. 2010. Microbial production of recalcitrant dissolved organic matter: long-term carbon storage in the global ocean. – Nat. Rev. Microbiol. 8: 593–599.
- Jover, L. F., Effler, T. C., Buchan, A., Wilhelm, S. W. and Weitz, J. S. 2014. The elemental composition of virus particles: implications for marine biogeochemical cycles. Nat. Rev. Microbiol. 12: 519–528.
- Keeling, M. J. and Rohani, P. 2008. Modeling infectious diseases in humans and animals. Princeton Univ. Press.
- Keesing, F., Holt, R. D. and Ostfeld, R. S. 2006. Effects of species diversity on disease risk. Ecol. Lett. 9: 485–498.
- Kermack, W. O., McKendrick, A. G. and Walker, G. T. 1927. A contribution to the mathematical theory of epidemics. – Proc. R. Soc. A 115: 700–721.
- Klawonn, I., Van den Wyngaert, S., Parada, A. E., Arandia-Gorostidi, N., Whitehouse, M. J., Grossart, H. P. and Dekas, A. E.

- 2021. Characterizing the "fungal shunt": parasitic fungi on diatoms affect carbon flow and bacterial communities in aquatic microbial food webs. Proc. Natl Acad. Sci. USA 118: 11.
- Knops, J. M. H. and Tilman, D. 2000. Dynamics of soil nitrogen and carbon accumulation for 61 years after agricultural abandonment. – Ecology 81: 88–98.
- Kohli, M., Borer, E. T., Kinkel, L. and Seabloom, E. W. 2019. Stability of grassland production is robust to changes in the consumer food web. – Ecol. Lett. 22: 707–716.
- Kohli, M., Henning, J. A., Borer, E. T., Kinkel, L. and Seabloom, E. W. 2021. Foliar fungi and plant diversity drive ecosystem carbon fluxes in experimental prairies. Ecol. Lett. 24: 487–497.
- Kuris, A. M., Blaustein, A. R. and Alio, J. J. 1980. Hosts as islands.
   Am. Nat. 116: 570–586.
- Leroy, C. J., Fischer, D. G., Halstead, K., Pryor, M., Bailey, J. K. and Schweitzer, J. A. 2011. A fungal endophyte slows litter decomposition in streams. Freshwater Biol. 56: 1426–1433.
- Lindeman, R. L. 1942. The trophic-dynamic aspect of ecology. Ecology 23: 399–418.
- Lønborg, C., Middelboe, M. and Brussaard, C. P. D. 2013. Viral lysis of *Micromonas pusilla*: impacts on dissolved organic matter production and composition. Biogeochemistry 116: 231–240.
- Loreau, M., Roy, J. and Tilman, D. 2005. Linking ecosystem and parasite ecology. In: Thomas, F., Renaud, F. and Guegan, J.-F. (eds), Parasitism and ecosystems. Oxford Univ. Press, pp. 13–21.
- Lovett, G. M., Arthur, M. A., Weathers, K. C. and Griffin, J. M. 2010. Long-term changes in forest carbon and nitrogen cycling caused by an introduced pest/pathogen complex. – Ecosystems 13: 1188–1200.
- Madden, L. V., Jeger, M. J. and van den Bosch, F. 2000. A theoretical assessment of the effects of vector-virus transmission mechanism on plant virus disease epidemics. Phytopathology 90: 576–594.
- May, R. M. and Anderson, R. M. 1979. Population biology of infectious diseases. 2. Nature 280: 455–461.
- May, R. M. and Nowak, M. A. 1994. Superinfection, metapopulation dynamics, and evolution of diversity. J. Theor. Biol. 170: 95–114.
- Miller, J. R. B., Ament, J. M. and Schmitz, O. J. 2014. Fear on the move: predator hunting mode predicts variation in prey mortality and plasticity in prey spatial response. J. Anim. Ecol. 83: 214–222.
- Mitchell, C. E. 2003. Trophic control of grassland production and biomass by pathogens. Ecol. Lett. 6: 147–155.
- Morowitz, H. J. 1968. Energy flow in biology: biological organization as a problem in thermal physics. Academic Press.
- Mur, L. A. J., Simpson, C., Kumari, A., Gupta, A. K. and Gupta, K. J. 2017. Moving nitrogen to the centre of plant defence against pathogens. – Ann. Bot. 119: 703–709.
- O'Halloran, L. R. et al. 2013. Regional contingencies in the relationship between aboveground biomass and litter in the world's grasslands. PLoS One 8: e54988.
- Oliva, J., Stenlid, J. and Martinez-Vilalta, J. 2014. The effect of fungal pathogens on the water and carbon economy of trees: implications for drought-induced mortality. New Phytol. 203: 1028–1035.
- Omacini, M., Chaneton, E. J., Ghersa, C. M. and Otero, P. 2004. Do foliar endophytes affect grass litter decomposition? A microcosm approach using *Lolium multiflorum*. – Oikos 104: 581–590.
- Ormeno, E., Baldy, V., Ballini, C., Larcheveque, M., Perissol, C. and Fernandez, C. 2006. Effects of environmental factors and leaf chemistry on leaf litter colonization by fungi in a Mediterranean shrubland. Pedobiologia 50: 1–10.

- Pastor, J. 2008. Mathematical ecology of populations and ecosystems. Wiley-Blackwell.
- Pazianoto, L. H. R., Solla, A. and Ferreira, V. 2019. Leaf litter decomposition of sweet chestnut is affected more by oomycte infection of trees than by water temperature. – Fungal Ecol. 41: 269–278.
- Pearl, R. and Reed, L. J. 1920. On the rate of growth of the population of the United States since 1790 and its mathematical representation. Proc. Natl Acad. Sci. USA 6: 275–288.
- Pell, B., Kendig, A. E., Borer, E. T. and Kuang, Y. 2019. Modeling nutrient and disease dynamics in a plant–pathogen system. – Math. Biosci. Eng. 16: 234–264.
- Preston, D. L., Mischler, J. A., Townsend, A. R. and Johnson, P. T. J. 2016. Disease ecology meets ecosystem science. Ecosystems 19: 737–748.
- Reich, P. B. 2014. The world-wide 'fast-slow' plant economics spectrum: a traits manifesto. J. Ecol. 102: 275–301.
- Rhodes, C. J. and Martin, A. P. 2010. The influence of viral infection on a plankton ecosystem undergoing nutrient enrichment. J. Theor. Biol. 265: 225–237.
- Rojas, C. M., Senthil-Kumar, M., Tzin, V. and Mysore, K. S. 2014. Regulation of primary plant metabolism during plant-pathogen interactions and its contribution to plant defense. – Front. Plant Sci. 5: 17.
- Roy, J., Saugier, B. and Mooney, H. A. 2001. Terrestrial global productivity. Academic Press.
- Ruardij, P., Veldhuis, M. J. W. and Brussaard, C. P. D. 2005. Modeling the bloom dynamics of the polymorphic phytoplankter Phaeocystis globosa: impact of grazers and viruses. – Harmful Algae 4: 941–963.
- Schlesinger, W. H. and Bernhardt, E. S. 2013. Biogeochemistry: an analysis of global change. Academic Press.
- Schwachtje, J., Fischer, A., Erban, A. and Kopka, J. 2018. Primed primary metabolism in systemic leaves: a functional systems analysis. Sci. Rep. 8: 216.
- Seabloom, E. W., Borer, E. T., Gross, K., Kendig, A. E., Lacroix, C., Mitchell, C. E., Mordecai, E. A. and Power, A. G. 2015. The community ecology of pathogens: coinfection, coexistence and community composition. – Ecol. Lett. 18: 401–415.
- Seabloom, E. W., Kinkel, L., Borer, E. T., Hautier, Y., Montgomery, R. A. and Tilman, D. 2017. Food webs obscure the strength of plant diversity effects on primary productivity. – Ecol. Lett. 20: 505–512.
- Seabloom, E. W., Borer, E. T., Hobbie, S. E. and MacDougall, A. S. 2021. Soil nutrients increase long-term soil carbon gains three-fold on retired farmland. Global Change Biol. 27: 4909–4920.
- Shaw, A. K., Peace, A., Power, A. G. and Bosque-Perez, N. A. 2017. Vector population growth and condition-dependent movement drive the spread of plant pathogens. – Ecology 98: 2145–2157.
- Shigesada, N. and Okubo, A. 1981. Analysis of the self-shading effect of algal vertical-distribution in natural waters. – J. Math. Biol. 12: 311–326.
- Shoemaker, L. G., Hayhurst, E., Weiss-Lehman, C. P., Strauss, A. T., Porath-Krause, A., Borer, E. T., Seabloom, E. W. and Shaw, A. K. 2019. Pathogens manipulate the preference of vectors, slowing disease spread in a multi-host system. Ecol. Lett. 22: 1115–1125.
- Strauss, A. T., Shoemaker, L. G., Seabloom, E. W. and Borer, E. T. 2019. Cross-scale dynamics in community and disease ecology:

- relative timescales shape the community ecology of pathogens. Ecology 100: 1–13.
- Strauss, A. T., Henning, J. A., Porath-Krause, A., Asmus, A. L., Shaw, A. K., Borer, E. T. and Seabloom, E. W. 2020. Vector demography, dispersal and the spread of disease: experimental epidemics under elevated resource supply. Funct. Ecol. 34: 2560–2570.
- Suttle, C. A. 2005. Viruses in the sea. Nature 437: 356–361.
- Suttle, C. A., Chan, A. M. and Cottrell, M. T. 1990. Infection of phytoplankton by viruses and reduction of primary productivity. – Nature 347: 467–469.
- Suttle, C. A. 2007. Marine viruses major players in the global ecosystem. Nat. Rev. Microbiol. 5: 801–812.
- Thingstad, T. F., Vage, S., Storesund, J. E., Sandaa, R. A. and Giske, J. 2014. A theoretical analysis of how strain-specific viruses can control microbial species diversity. Proc. Natl Acad. Sci. USA 111: 7813–7818.
- Townsend, D. W., Cammen, L. M., Holligan, P. M., Campbell, D.
  E. and Pettigrew, N. R. 1994. Causes and consequences of variability in the timing of spring phytoplankton blooms. –
  Deep-Sea Res. Part I: Oceanogr. Res. Pap. 41: 747–765.
- Turner, W. C., Kausrud, K. L., Krishnappa, Y. S., Cromsigt, J., Ganz, H. H., Mapaure, I., Cloete, C. C., Havarua, Z., Kusters, M., Getz, W. M. and Stenseth, N. C. 2014. Fatal attraction: vegetation responses to nutrient inputs attract herbivores to infectious anthrax carcass sites. Proc. R. Soc. B 281: 20141785.
- Ulanowicz, R. E. 1972. Mass and energgy flow in closed ecosystems. J. Theor. Biol. 34: 239–253.
- Vage, S., Pree, B. and Thingstad, T. F. 2016. Linking internal and external bacterial community control gives mechanistic framework for pelagic virus-to-bacteria ratios. – Environ. Microbiol. 18: 3932–3948.
- van der Valk, A. G. 1986. The impact of litter and annual plants on recruitment from the seed bank of a lacustrine wetland. Aquat. Bot. 24: 13–26.
- Verelst, F., Willem, L. and Beutels, P. 2016. Behavioural change models for infectious disease transmission: a systematic review (2010–2015). J. R. Soc. Interface 13: 20160820.
- Verhulst, P.-F. 1845. Recherches mathématiques sur la loi d'accroissement de la population. Nouv. Mém. Acad. R. Sci. Bruxelles 18: 1–41.
- Weil, R. R. and Magdoff, F. 2004. Significance of soil organic matter to soil quality and health. CRC Press Inc., pp. 1–43.
- Weitz, J. S. and Wilhelm, S. W. 2012. Ocean viruses and their effects on microbial communities and biogeochemical cycles. F1000 Biol. Rep. 4: 17–17.
- Weitz, J. S., Stock, C. A., Wilhelm, S. W., Bourouiba, L., Coleman, M. L., Buchan, A., Follows, M. J., Fuhrman, J. A., Jover, L. F., Lennon, J. T., Middelboe, M., Sonderegger, D. L., Suttle, C. A., Taylor, B. P., Thingstad, T. F., Wilson, W. H. and Wommack, K. E. 2015. A multitrophic model to quantify the effects of marine viruses on microbial food webs and ecosystem processes. ISME J. 9: 1352–1364.
- Wilhelm, S. W. and Suttle, C. A. 1999. Viruses and nutrient cycles in the sea: viruses play critical roles in the structure and function of aquatic food webs. Bioscience 49: 781–788.
- Wolfe, E. R. and Ballhorn, D. J. 2020. Do foliar endophytes matter in litter decomposition? Microorganisms 8: 446.
- Wright, I. J. et al. 2004. The worldwide leaf economics spectrum. Nature 428: 821–827.